

SuperSolver: accelerating the Delfs–Galbraith algorithm with fast subfield root detection

Maria Corte-Real Santos^{1*}, Craig Costello², and Jia Shi^{3†}

¹ University College London, London, UK
maria.santos.20@ucl.ac.uk

² Microsoft Research, Redmond, USA
craigco@microsoft.com

³ University of Waterloo, Waterloo, Canada
j96shi@uwaterloo.ca

Abstract. We give a new algorithm for finding an isogeny from a given supersingular elliptic curve E/\mathbb{F}_{p^2} to a subfield elliptic curve E'/\mathbb{F}_p , which is the bottleneck step of the Delfs–Galbraith algorithm for the general supersingular isogeny problem. Our core ingredient is a novel method of rapidly determining whether a polynomial $f \in L[X]$ has any roots in a subfield $K \subset L$, while avoiding expensive root-finding algorithms. In the special case when $f = \Phi_{\ell,p}(X, j) \in \mathbb{F}_{p^2}[X]$, i.e., when f is the ℓ -th modular polynomial evaluated at a supersingular j -invariant, this provides a means of efficiently determining whether there is an ℓ -isogeny connecting the corresponding elliptic curve to a subfield curve. Together with the traditional Delfs–Galbraith walk, inspecting many ℓ -isogenous neighbours in this way allows us to search through a larger proportion of the supersingular set per unit of time. Though the asymptotic $\tilde{O}(p^{1/2})$ complexity of our improved algorithm remains unchanged from that of the original Delfs–Galbraith algorithm, our theoretical analysis and practical implementation both show a significant reduction in the runtime of the subfield search. This sheds new light on the concrete hardness of the general supersingular isogeny problem, the foundational problem underlying isogeny-based cryptography.

Keywords: Isogeny-based cryptography, supersingular isogeny problem, Delfs–Galbraith algorithm.

1 Introduction

In its most general form, the *supersingular isogeny problem* asks to find an isogeny

$$\phi: E_1 \rightarrow E_2$$

between two given supersingular curves, $E_1/\bar{\mathbb{F}}_p$ and $E_2/\bar{\mathbb{F}}_p$. The best known classical attack against the supersingular isogeny problem is the Delfs–Galbraith algorithm [9], which, in the general case where E_1 and E_2 are curves defined over \mathbb{F}_{p^2} , has two steps. The first step computes random walks in the ℓ -isogeny graph (for some choice of ℓ) to find isogenies $\phi_1: E_1 \rightarrow E'_1$ and $\phi_2: E_2 \rightarrow E'_2$, such that E'_1/\mathbb{F}_p and E'_2/\mathbb{F}_p are *subfield curves*. There are around $\lfloor p/12 \rfloor$ supersingular curves up to isomorphism and $O(p^{1/2})$ of them are subfield curves, therefore this step runs in $\tilde{O}(p^{1/2})$ bit operations. The second step searches for a *subfield* isogeny $\phi': E'_1 \rightarrow E'_2$ that connects ϕ_1 and ϕ_2 , and it requires $\tilde{O}(p^{1/4})$ bit operations [9]. It follows that the entire algorithm runs in $\tilde{O}(p^{1/2})$ operations on average, with the cost dominated by the first step, i.e., the search for paths to subfield curves.

*Supported by EPSRC grant EP/S022503/1.

†Part of this work was done while Jia was an intern at Microsoft Research.

Solver. To our knowledge, a precise complexity analysis of the Delfs–Galbraith algorithm has not been conducted. We fill this gap by presenting an optimised implementation of the Delfs–Galbraith algorithm, called **Solver**, and conducting experiments over many thousands of instances of the subfield search problem to determine its concrete complexity. Though **Solver** finds the full path, we focus on the optimisation and complexity of the bottleneck step: finding subfield curves. These optimisations include:

- *Choice of ℓ .* In their high-level description of the algorithm, Delfs and Galbraith do not specify which ℓ -isogeny graph to walk in. Framing the problem of taking a step in the ℓ -isogeny graph as computing the roots of a polynomial of degree ℓ , in **Solver** we chose the simplest and most efficient choice: $\ell = 2$.
- *Fast square root finding in \mathbb{F}_{p^2} .* We use the techniques presented in [21, §5.3] to construct an optimised algorithm for finding square roots in \mathbb{F}_{p^2} , which only requires two \mathbb{F}_p exponentiations and a few \mathbb{F}_p multiplications and additions.
- *Random walks in the 2-isogeny graph.* We implement a depth-first search to find subfield nodes in the 2-isogeny graph and give a precise complexity analysis on the number of \mathbb{F}_p operations required.

SuperSolver. The main contribution of this paper is a new state-of-the-art algorithm for solving the general supersingular isogeny problem, called **SuperSolver**. This is a variant of the Delfs–Galbraith algorithm that exploits a combination of our new *subfield root detection* algorithm and the use of modular polynomials. We show that we can efficiently determine whether a polynomial $f \in L[X]$ has a root in a subfield $K \subset L$, without finding any roots explicitly. Though this algorithm works for general fields and polynomials (and may be of use in other contexts), we apply it to the case where $f = \Phi_{\ell,p}(X, j) \in \mathbb{F}_{p^2}[X]$, i.e., where f is the ℓ -th modular polynomial evaluated at a supersingular j -invariant. This provides a means of quickly determining whether there is an ℓ -isogeny connecting the corresponding elliptic curve to a subfield curve: we develop this `NeighbourInFp` subroutine in Section 4, and use it as the core of our **SuperSolver** algorithm in Section 5.

In Section 7, we conduct extensive experiments using both our **Solver** and **SuperSolver** libraries, all of which show that **SuperSolver** performs much faster than **Solver**. In Table 1, we give a taste of the types of improvements we see in searching for subfield nodes over supersingular sets of various sizes, taking a number of primes from the isogeny-based literature. These primes were specifically chosen because the Delfs–Galbraith algorithm for the general supersingular isogeny problem is the best known classical attack against the cryptosystems they target.

Our **Solver** and **SuperSolver** algorithms are written in Sage [26] and Python and can be found at

<https://github.com/microsoft/SuperSolver>.

Cryptographic implications. This paper has implications on the classical bit-security of any supersingular isogeny-based scheme for which the Delfs–Galbraith algorithm is the best known attack; this includes the key exchange scheme B-SIDH [6], the signature scheme in [12, §4], and the signature scheme SQISign [11]. For any proposed instantiation of such schemes, our **SuperSolver** suite allows the analysis in Section 7 to be conducted on input of any prime p , and determines a precise estimate on the number of operations required (on average) to solve the corresponding supersingular isogeny problem. This is especially accurate when the cardinality of the class group is known, which has recently been shown to be feasible for primes up to 512 bits [3]. On the other hand, we point out that the improvements in this paper have no direct impact on the classical security of SIDH [10] and SIKE [15]. Though the Delfs–Galbraith algorithm can be used to attack any supersingular isogeny-based cryptosystem, there are much faster *claw-finding* algorithms (see [10]) for solving the special instances of isogeny problems that arise in those schemes.

prime p	Solver	SuperSolver		
B-SIDH-p247 [6]	246,461 (406)	{3,5,7,11,13} 1,726,427 (58.0)	{3,5,7,11,13,9} 1,723,345 (58.1)	{3,5,7,11} 1,711,713 (58.5)
TwinSmooth-p250 [8]	233,511 (430)	{3,5,7,11,13,9} 1,699,825 (59.1)	{3,5,7,11,13} 1,697,769 (59.1)	{3,5,7,11,9} 1,680,379 (59.8)
SQISign-p256 [11]	246,459 (407)	{3,7,5,11,13} 1,726,427 (58.0)	{3,7,5,11,13,9} 1,723,345 (58.1)	{3,7,5,11} 1,711,713 (58.5)
TwinSmooth-p384 [8]	163,331 (610)	{3,5,7,11,13,9} 1,529,025 (65.2)	{3,5,7,11,13} 1,494,725 (66.6)	{3,5,7,11,13,9,17} 1,487,919 (67.0)
TwinSmooth-p512 [8]	127,511 (786)	{3,5,4,7,11,13,9,8} 1397761 (71.7)	{3,5,4,7,11,13,9} 1391645 (72.0)	{3,5,4,7,11,13,9,8,17} 1355575 (73.9)

Table 1. The number of nodes inspected per 10^8 field multiplications for primes targeting schemes where Delfs–Galbraith is the best known classical attack. The Solver column corresponds to optimised Delfs–Galbraith walks in $\mathcal{X}(\mathbb{F}_p, 2)$ – see Section 3. The SuperSolver columns correspond to enabling our fast subfield root detection algorithm with the three fastest sets of ℓ ’s (left to right) – see Section 5. Numbers in round brackets are the approximate number of \mathbb{F}_p multiplications per node inspected at each step, as computed during the precomputation phase that predicts which sets of ℓ ’s will perform fastest.

Roadmap. We give the preliminaries in Section 2. In Section 3, we present our optimised instantiation of the traditional Delfs–Galbraith algorithm, called Solver. In Section 4, we construct an efficient algorithm to detect whether a polynomial has a root in a subfield. We use this algorithm to build SuperSolver in Section 5. In Section 6, we present a worked example to highlight the differences between both algorithms, and in Section 7 we present a number of implementation results that illustrate the concrete improvements offered by SuperSolver.

2 Preliminaries

In this section we briefly set notation and give the requisite background for this paper. Readers familiar with the paragraph headings below are welcome to skip to the final two paragraphs.

Modular polynomials. We will use $\Phi_\ell(X, Y) \in \mathbb{Z}[X, Y]$ to denote the classical modular polynomial (see [25]) that parameterises pairs of elliptic curves with cyclic ℓ -isogeny in terms of their j -invariants: $\Phi_\ell(j_1, j_2) = 0$ if and only if j_1 and j_2 are the j -invariants of ℓ -isogenous elliptic curves. Readers unfamiliar with modular polynomials are encouraged to look at Sutherland’s database⁴, which contains $\Phi_\ell(X, Y)$ for all $\ell \leq 300$ and for all primes $\ell \leq 1000$. The polynomial Φ_ℓ is symmetric in X and Y , i.e., $\Phi_\ell(X, Y) = \Phi_\ell(Y, X)$, and if $\ell = \prod_{i=1}^n \ell_i^{e_i}$ is ℓ ’s prime decomposition, the degree of $\Phi_\ell(X, Y)$ in both X and Y is

$$N_\ell := \deg(\Phi_\ell(X, Y)) = \prod_{i=1}^n (\ell_i + 1) \ell_i^{e_i - 1}. \quad (1)$$

The difficulty in computing $\Phi_\ell(X, Y)$ is in the size, rather than the number, of its coefficients. As discussed in [25], storing $\Phi_\ell(X, Y)$ requires $O(\ell^3 \log \ell)$ bits, which corresponds to several gigabytes for $\ell \approx 1000$ and many terabytes for $\ell \approx 10^4$. Fortunately, for our purposes, the modular polynomials already contained in Sutherland’s database are more than sufficient. Moreover, we will be using them in the context of cryptanalysing instances of the supersingular isogeny problem over a fixed finite field \mathbb{F}_{p^2} , meaning we can reduce all of the large coefficients modulo p as a precomputation. Indeed, even before the target j -invariants are known, $\Phi_\ell(X, Y) \in \mathbb{Z}[X, Y]$ will be preprocessed into

$$\Phi_{\ell,p}(X, Y) \in \mathbb{F}_p[X, Y],$$

where we note the additional subscript, defined by reducing all coefficients of $\Phi_\ell(X, Y)$ modulo p . By the symmetry of $\Phi_\ell(X, Y)$, this means we must store around $N_\ell^2/2$ coefficients in \mathbb{F}_p , requiring only $O(\ell^2 \log p)$ bits.

⁴See [24], a database computed using techniques from various joint works of his [25,4].

Supersingular isogeny graphs. Following [9, §1], let $p > 3$ be a prime and let S_{p^2} denote the set of all supersingular j -invariants in \mathbb{F}_{p^2} . The number of such j -invariants is $\#S_{p^2} = \lfloor p/12 \rfloor + b$, where $b \in \{0, 1, 2\}$ is determined by the value of $p \bmod 12$ [23, Theorem V.4.1(c)]. For any ℓ with $p \nmid \ell$, we use $\mathcal{X}(\overline{\mathbb{F}}_p, \ell)$ to denote the *supersingular isogeny graph* whose nodes correspond to the j -invariants in S_{p^2} and whose edges are ℓ -isogenies defined over $\overline{\mathbb{F}}_p$. These graphs are fully connected for every prime ℓ [19], and (with the possible exception of a few nodes) are $(\ell+1)$ -regular expander graphs that satisfy the Ramanujan property [20]. Crucial to both the Delfs–Galbraith algorithm and this paper is the subset S_p of supersingular j -invariants defined over \mathbb{F}_p . The size of this set is $\#S_p = \tilde{O}(p^{1/2})$ [9, Equation 1], and since $\#S_{p^2} = O(p)$, the expected number of randomly chosen elements in S_{p^2} we would have to take before finding one in S_p is in $\tilde{O}(p^{1/2})$.

The Delfs–Galbraith algorithm. The Delfs–Galbraith paper largely focusses on the problem of finding an isogeny $\phi': E'_1 \rightarrow E'_2$ between two supersingular curves, E'_1/\mathbb{F}_p and E'_2/\mathbb{F}_p , whose j -invariants are in S_p . One of their main results is an algorithm [9, Algorithm 1] that computes such a ϕ' in $\tilde{O}(p^{1/4})$ bit operations. At the end of their paper [9, Section 4], they show how this can be used as a subroutine to give an algorithm for the general supersingular isogeny problem, which asks to find an isogeny

$$\phi: E_1 \rightarrow E_2$$

between two supersingular curves, E_1/\mathbb{F}_{p^2} and E_2/\mathbb{F}_{p^2} , whose j -invariants are in S_{p^2} . The idea is to perform simple self-avoiding random walks in $\mathcal{X}(\overline{\mathbb{F}}_p, \ell)$ until hitting an elliptic curve with a j -invariant defined over \mathbb{F}_p . Finding a walk from E_1/\mathbb{F}_{p^2} to E'_1/\mathbb{F}_p yields an isogeny $\psi_1: E_1 \rightarrow E'_1$, and finding a walk from E_2/\mathbb{F}_{p^2} to E'_2/\mathbb{F}_p yields an isogeny $\psi_2: E_2 \rightarrow E'_2$. A full isogeny $\phi: E_1 \rightarrow E_2$ is then found as the composition $\phi = (\hat{\psi}_2 \circ \phi' \circ \psi_1)$, where $\hat{\psi}_2: E'_2 \rightarrow E_2$ is the dual of ψ_2 , and $\phi': E'_1 \rightarrow E'_2$ is the subfield isogeny above that can be computed in $\tilde{O}(p^{1/4})$ bit operations. The bottleneck in the Delfs–Galbraith algorithm is finding the paths from the curves with $j \in S_{p^2} \setminus S_p$ to the curves with $j \in S_p$. From the above discussion, the number of j -invariants in S_{p^2} we expect to search over before finding one in S_p is $\tilde{O}(p^{1/2})$. Following [9, Section 4], the steps taken in $\mathcal{X}(\overline{\mathbb{F}}_p, \ell)$ are self-avoiding, meaning that one stores the current j -invariant, j_c , and the previous j -invariant j_p . To take the next step, one then chooses one of the $N_\ell - 1$ roots (see Equation 1) of

$$\Phi_\ell(X, j_c)/(X - j_p)$$

at random. Since ℓ and N_ℓ are fixed and small, it follows that the asymptotic complexity of the search for subfield j -invariants is $\tilde{O}(p^{1/2})$. Before presenting our improved search for subfield j -invariants, in Section 3 we present an optimised version of this algorithm, and subsequently replace the \tilde{O} above with a precise, concrete complexity.

Factoring polynomials in finite fields. Let $f(X) \in \mathbb{F}_q[X]$ be a monic polynomial of degree ℓ with $q = p^k$ for a prime p , and for the purposes of this paper, assume that p is very large (i.e., cryptographically sized) and ℓ is relatively small (i.e., $\ell < 100$). The literature contains a number of methods for finding the irreducible factors of f in $\mathbb{F}_q[x]$, and we briefly mention the most applicable and well-known algorithms for our scenario. Berlekamp’s algorithm [2] factors f using an expected number of $O(\ell^3 + \ell^2 \log \ell \log q)$ operations in \mathbb{F}_q [22, Theorem 20.12]. This appears to be superior to the Cantor–Zassenhaus algorithm [5], which uses an expected number of $O(\ell^3 \log q)$ operations in \mathbb{F}_q [22, Theorem 20.9], however one can take advantage of certain time-memory trade-offs to implement Cantor–Zassenhaus so that it requires $O(\ell^3 + \ell^2 \log q)$ operations in \mathbb{F}_q [22, Exercise 20.13]. Note that both of these big- O complexities hide a number of subtleties, that \mathbb{F}_q -inversions are included as \mathbb{F}_q operations, and moreover that both of these algorithms are probabilistic. Their deterministic variants have worse complexities [22, §20.6].

Polynomial GCD. Euclid’s integer GCD algorithm is easily adapted to compute polynomial GCD’s [22, §17.3]. Computing the GCD of two polynomials $g, h \in \mathbb{F}_q[x]$ requires $O(\deg(g) \cdot \deg(h))$

operations in \mathbb{F}_q . Again, here each \mathbb{F}_q inversion is counted as an \mathbb{F}_q operation. In order to make our algorithms run as fast as possible, one of the necessary subroutines we derive in Section 4 is an inversion-free polynomial GCD algorithm, for which we state a tight upper bound on the concrete complexity.

Measuring complexity. Throughout this paper we will avoid stating asymptotic (i.e., big- O -style) complexities in favour of stating concrete ones. One of our goals in Section 3 is to replace the $\tilde{O}(p^{1/2})$ complexity of the original Delfs–Galbraith algorithm with a closed formula that can be used to give precise estimates on the classical security of the relevant cryptographic instantiations. We will use the metric of \mathbb{F}_p multiplications as convention, noting that it is relatively straightforward to convert this into a more fine-grained metric (e.g. bit operations, machine operations, cycle counts, gate counts, circuit depth, etc.) depending on the context and on the implementation of the \mathbb{F}_p arithmetic. For simplicity, we will count \mathbb{F}_p squarings as multiplications and ignore additions. We justify this by noting that, roughly speaking, the ratio of multiplications to additions in all of the algorithms in this work are similar, and the complexity of \mathbb{F}_p additions have a minimal impact on any of the aforementioned metrics.

Subfield search complexity determines concrete bit security. Both the Solver implementation detailed in Section 3 and the SuperSolver implementation detailed in Section 5 solve *all* instances of the general supersingular isogeny problem. On input of any prime p and any two supersingular j -invariants in S_{p^2} , both implementations will always terminate with an isogeny that solves the corresponding problem. We emphasise that henceforth our sole focus is on the $\tilde{O}(p^{1/2})$ subfield search phase of the Delfs–Galbraith algorithm. Finding a path between subfield nodes requires $\tilde{O}(p^{1/4})$ operations, which is negligible in both the asymptotic sense and in the sense of obtaining cryptographic security estimates. To see this, suppose the asymptotic $\tilde{O}(p^{1/2})$ complexity of the first phase is replaced by a concrete complexity of $c_p \cdot p^{1/2}$, and the asymptotic $\tilde{O}(p^{1/4})$ complexity of the second phase is replaced by a concrete complexity of $d_p \cdot p^{1/2}$, where c_p and d_p are polynomials in $\log p$. The total complexity of the Delfs–Galbraith algorithm is then

$$c_p \cdot p^{1/2} + d_p \cdot p^{1/4}.$$

For primes of cryptographic size, small changes in c_p have an immediate influence on the total runtime of the algorithm, while much larger changes in d_p will not play a part in the bit security of the problem. For $p > 2^{200}$, a factor 2 change in c_p changes the bit security of the problem by 1, while d_p would have to change by a factor of at least 2^{50} to have the same impact on the bit security.

3 Solver: optimised Delfs–Galbraith subfield searching in $\mathcal{X}(\overline{\mathbb{F}}_p, 2)$

Recall from the previous section that the self-avoiding walks in $\mathcal{X}(\overline{\mathbb{F}}_p, \ell)$ store the current j -invariant, j_c , and the previous j -invariant j_p , and then take a step in $\mathcal{X}(\overline{\mathbb{F}}_p, \ell)$ by choosing one of the $N_\ell - 1$ roots of $\Phi_\ell(X, j_c)/(X - j_p)$. In determining the asymptotic $\tilde{O}(p^{1/2})$ complexity of these walks, Delfs and Galbraith did not need to analyse the cost of a single step. However, to set the stage for our improved search in Section 5, we must optimise this process and determine its concrete cost. The first parameter that must be specified is ℓ , i.e., the isogeny graph to walk around in. Considering both Equation (1) and the complexity of the factorisation algorithms in Section 2, we chose $\ell = 2$ to obtain most efficient and simplest choice where we are able to take advantage of fast explicit methods for computing square roots in \mathbb{F}_{p^2} .

Scott’s fast square roots in \mathbb{F}_{p^2} . Optimal computation of square roots in extension fields of large characteristic requires careful attention to detail. A 2013 paper by Adj and Rodríguez-Henríquez [1] cost the process of computing square roots in \mathbb{F}_{p^2} at two \mathbb{F}_p residuosity tests, two

\mathbb{F}_p square roots, and one \mathbb{F}_p inversion, for a total of five exponentiations in \mathbb{F}_p . In [21, §5.3], Scott shows that these operations can be combined in a clever way to significantly reduce this cost. The inputs into the Tonelli-Shanks \mathbb{F}_p square root algorithm [18, Algorithm 3.34] can be tweaked in such a way that the two residuosity tests are absorbed into the two square roots. Moreover, he shows that most of the inversion cost can also be absorbed by application of Hamburg’s combined ‘square-root-and-inversion’ trick [13]. This reduces the bulk of cost of an \mathbb{F}_{p^2} square root from five \mathbb{F}_p exponentiations to just two. In addition, there are a handful of \mathbb{F}_p multiplications and additions that either update the Tonelli-Shanks outputs depending on the residuosity outcomes or collect and combine the results according to the ‘complex’ formula in [21, §5.3]. We use this to construct a general square root algorithm in our implementation that is highly optimised with respect to the number of \mathbb{F}_p operations it incurs⁵.

Taking a step in $\mathcal{X}(\overline{\mathbb{F}}_p, 2)$. After stepping from $j_p \in \mathbb{F}_{p^2}$ to $j_c \in \mathbb{F}_{p^2}$, a self-avoiding walk in $\mathcal{X}(\overline{\mathbb{F}}_p, 2)$ will step to one of two new nodes: j_0 and j_1 . These are computed by solving the quadratic equation that arises from the modular polynomial $\Phi_\ell(X, Y)$ with $\ell = 2$:

$$\begin{aligned} \Phi_2(X, Y) = & -X^2Y^2 + X^3 + Y^3 + 1488 \cdot (X^2Y + Y^2X) - 162000 \cdot (X^2 + Y^2) \\ & + 40773375 \cdot XY + 8748000000 \cdot (X + Y) - 157464000000000. \end{aligned}$$

The three neighbours of j_c in $\mathcal{X}(\overline{\mathbb{F}}_p, 2)$ are j_p , j_0 , and j_1 , meaning that $\Phi_2(X, j_c)$ factorises as

$$\Phi_2(X, j_c) = (X - j_p)(X - j_0)(X - j_1).$$

This yields a quadratic equation, whose solutions are j_0, j_1 , defined by $AX^2 + BX + C = 0$ where

$$\begin{aligned} A &= -(j_p + j_0 + j_1) + j_c^2 - 1488j_c + 162000, \\ B &= -1488j_c^2 - 40773375j_c + (j_1 + j_p)j_0 + j_1j_p - 8748000000, \quad \text{and} \\ C &= -j_0j_1j_p - j_c^3 + 162000j_c^2 - 8748000000j_c + 157464000000000. \end{aligned}$$

Computing these coefficients costs a small, constant number of \mathbb{F}_p operations, so the process of computing j_0 and j_1 from j_p and j_c boils down to solving the quadratic equation, which essentially requires one \mathbb{F}_{p^2} square root. Since this square root incurs two \mathbb{F}_p exponentiations and a few additional \mathbb{F}_p operations, it follows that the cost of computing each new $j \in S_{p^2}$ during the walks in $\mathcal{X}(\overline{\mathbb{F}}_p, 2)$ is (on average) approximately one \mathbb{F}_p exponentiation.

The depth first search in $\mathcal{X}(\overline{\mathbb{F}}_p, 2)$. Repeating the process described above allows us to perform the search for subfield nodes using a depth first search in a binary tree with d levels as follows. We write $j_{m,n}$ for the n -th node at level m , where $0 \leq m \leq d$ and $0 \leq n \leq 2^m - 1$. The first three levels are depicted in Figure 1. We initialise the root node $j_{0,0}$ as the target $j \in S_{p^2}$, and set $j_{1,0}$ and $j_{1,1}$ as two of its three neighbours⁶ in $\mathcal{X}(\overline{\mathbb{F}}_p, 2)$. The depth first search starts by setting $j_c = j_{1,0}$ and $j_p = j_{0,0}$. We then solve the quadratic equation above to obtain $j_{2,0}$ and $j_{2,1}$, and repeat this procedure with $j_c = j_{i+1,0}$ and $j_p = j_{i,0}$ for $1 \leq i \leq d - 1$ until the leftmost leaf $j_{d,0}$ is computed and the `path` stack is fully initialised as

$$\text{path} = [j_{0,0}, j_{1,0}, \dots, j_{d-1,0}, j_{d,0}].$$

To avoid any waste, we also maintain a stack of the other solution to the quadratic equations that were computed along the way, which we call sibling nodes

$$\text{siblings} = [j_{1,1}, \dots, j_{d-1,1}, j_{d,1}].$$

⁵Note that the fixed exponentiations that take place in the calls to Tonelli-Shanks could be further optimised for a specific p by tailoring a larger window or a different addition chain, but the impact (for our purposes and comparisons) of this improvement would be minor.

⁶Initially we do not have a j_p , so all three neighbours can be computed using generic root finding; our code does this during the setup phase.

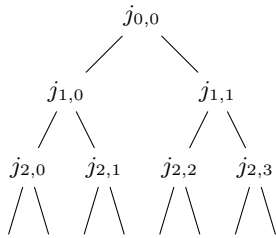


Fig. 1. Levels 0, 1, and 2 of the binary tree in the depth first search of $\mathcal{X}(\bar{\mathbb{F}}_p, 2)$.

The algorithm then proceeds back up the levels by popping `path` until its last element is the root of a subtree that has not been checked in its entirety. At this point `siblings` is popped and pushed into `path`. When the last element of `path` is the root of a subtree that has not been exhausted, we initialise the process of solving quadratic equations, pushing one of the two solutions into `path` and the other into `siblings` until `path` contains $d + 1$ elements. Each time the quadratic equation solver is called, the two roots (i.e., j -invariants) are immediately checked; if either of them lie in \mathbb{F}_p , it is added to `path` and the process is terminated. Otherwise, the process is repeated recursively until `path` = $[j_{0,0}]$, in which case the $2^{d+1} - 1$ nodes in the tree have been exhausted without finding a solution. To guarantee that a solution is found, one could increase d and start again, but our code proceeds by simply storing the first (leftmost) leaf and its parent in separate memory so that the process can restart here and avoid recomputing any prior j 's. As Delfs and Galbraith point out, setting the depth $d = \frac{1}{2} \log_2 p$ should be enough. Since the number of nodes in the tree is 2^d , increasing d by ϵ makes the failure probability diminish by $1/2^\epsilon$. Setting $\epsilon = 10$ was sufficient in all of our experiments. Finally, as pointed out by Delfs and Galbraith in [9, §4], this process parallelises perfectly. For P processors, one can simply compute a binary tree of depth $\lceil \log_2 P \rceil$ during setup and distribute P of the leaf nodes as individual starting points.

The concrete complexity of Delfs–Galbraith. Table 2 reports on experiments conducted using `Solver`, the optimised instantiation of the traditional Delfs–Galbraith walk. For each bitlength between 21 and 40, we solved 10,000 instances of the subfield search. In each case we chose 100 random primes and, for each prime, 100 pseudo-random j -invariants in S_{p^2} . The numbers in each column report the averages (as base-2 logarithms) of these search complexities. In all cases the

bitlengths of primes p	21	22	23	24	25	26	27	28	29	30
av. number of nodes visited	8.8	9.4	10.0	10.3	10.9	11.4	11.9	12.3	13.1	13.5
av. number of \mathbb{F}_p multiplications	14.5	15.0	15.7	16.0	16.7	17.2	17.8	18.2	19.0	19.5
bitlengths of primes p	31	32	33	34	35	36	37	38	39	40
av. number of nodes visited	13.5	14.2	14.7	15.3	15.8	16.3	17.1	17.3	17.6	18.1
av. number of \mathbb{F}_p multiplications	19.5	20.5	20.8	21.3	21.9	22.4	23.2	23.6	24.1	24.6

Table 2. The concrete cost of the subfield search phase of the Delfs–Galbraith over small fields of various bitlengths. Further explanation in text.

number of \mathbb{F}_p multiplications is found to be

$$\#(\mathbb{F}_p \text{ muls.}) = c \cdot \sqrt{p} \cdot \log_2 p,$$

with $0.75 \leq c \leq 1.05$. In Section 7, we shed more light on the concrete complexity of both `Solver` and `SuperSolver`.

Remark 1. There is no traditional elliptic curve arithmetic found in either Solver or SuperSolver. All of the steps taken within $\mathcal{X}(\overline{\mathbb{F}}_p, 2)$ and the rapid inspections conducted in $\mathcal{X}(\overline{\mathbb{F}}_p, \ell)$ use the modular polynomials. We point out there *may* be specific instances of p where one could perform walks faster than repeatedly solving the $\Phi_{2,p}(X, j)$ quadratic by, say, employing Vélú's formulas [27] with the optimal strategies of De Feo–Jao–Plût [10]. For example, with a prime $p = 2^e 3^f - 1$, the price of computing a 2^e -isogeny (i.e., walking through e nodes in $\mathcal{X}(\overline{\mathbb{F}}_p, 2)$) in this way may be cheaper than the price of computing e square roots in \mathbb{F}_{p^2} (note that the latter reveals 2 nodes each time). However, we argue that these scenarios are likely to only exist for special instances of the supersingular isogeny problem that are geared towards cryptosystems like SIDH [10] and SIKE [15]. As discussed in Section 1, here there are claw-finding algorithms that are much faster than the Delfs–Galbraith algorithm (though the number of \mathbb{F}_p operations required to compute an ℓ^e -isogeny still grows with p , and therefore our fast subfield root detection would also be useful in that context). In the case of both general primes and the types of primes in Table 1, it is highly unlikely that using Vélú's formulas [27] will be competitive with the binary tree depth-first search in $\mathcal{X}(\overline{\mathbb{F}}_p, 2)$. Computing general $(\prod \ell_i^{e_i})$ -isogenies from kernel elements is much more expensive than ℓ^e -isogenies when $\ell \in \{2, 3\}$, and one covers fewer nodes in S_{p^2} per isogeny when the ℓ_i grow larger.

4 Fast subfield root detection

In this section we derive a method for determining whether a polynomial $f(X) = a_n X^n + \dots + a_1 X + a_0 \in \mathbb{F}_{q^d}[X]$ with $d \geq 2$ has a root lying in the subfield \mathbb{F}_q , where q is a power of prime p . Though this can be achieved by factoring the polynomial, the methods described in Section 2 become too costly for our purposes; the number of \mathbb{F}_q operations required depends on the size of q , which hampers their relative efficiency as q grows large. Our aim in this section is to detail a much faster algorithm that detects whether a root lies in a subfield and show that the number of \mathbb{F}_q operations required by our algorithm only depends on the degree of f and the degree of the extension d .

As the algorithms in this section may be of independent interest, we leave them as general as possible before specialising back to the application at hand in Section 5. The results up to Proposition 1 are presented for general finite field extensions of the form $\mathbb{F}_{q^d}/\mathbb{F}_q$, but we will later specialise to the quadratic extensions of prime fields, i.e., where $q = p$ and $d = 2$. The inversion-free GCD in Algorithm 1 is derived for an arbitrary polynomial ring $K[x]$, but we will only need to use it in $\mathbb{F}_p[x]$.

In this section, for a polynomial in $\mathbb{F}_{q^d}[X]$, we will reduce the the problem of detecting a root in \mathbb{F}_q to computing the greatest common divisor of d related polynomials g_1, \dots, g_d . In the case where $d > 2$, we will need to compute the GCD of more than two polynomials. This can be done by recursively computing the GCD of two polynomials and using the following identity:

$$\gcd(g_1, g_2, \dots, g_d) = \gcd(g_1, \gcd(g_2, \dots, g_d)). \quad (2)$$

We aim to minimise the number of \mathbb{F}_q multiplications needed to compute the GCD and so we construct these polynomials so that they are defined over \mathbb{F}_q . To achieve this, we will need two results. The first is a theorem by Lidl and Niederreiter [17, Theorem 2.24].

Theorem 1. *Let F be a finite extension of a finite field K , both considered as vector spaces over K . Then the linear transformations from F into K are exactly the mappings $L_\beta(\alpha)$, for $\beta \in F$, where $L_\beta(\alpha) = \text{Tr}_{F/K}(\beta\alpha)$ for all $\alpha \in F$. Furthermore, we have $L_\beta \neq L_\gamma$ whenever β, γ are distinct elements of F .*

The second result we will need is the following lemma.

Lemma 1. *Let $f_1, \dots, f_d \in \mathbb{F}_{q^d}[X]$ be polynomials and $A \in \text{GL}_d(\mathbb{F}_{q^d})$. Defining $(g_1, \dots, g_d) := A \cdot (f_1, \dots, f_d)$, we have*

$$\gcd(f_1, \dots, f_d) = \gcd(g_1, \dots, g_d).$$

Proof. If a polynomial $h \in \mathbb{F}_{q^d}[X]$ divides f_1, \dots, f_d , then h divides any linear combination of the f_1, \dots, f_d . Therefore, h divides g_1, \dots, g_d . Since A is invertible, by swapping the roles of g_i and f_i we see that the converse holds. \square

We are now ready to present the main result of this section.

Proposition 1. *For some $d \geq 2$, let π be the q -power Frobenius endomorphism in $\text{Gal}(\mathbb{F}_{q^d}/\mathbb{F}_q)$ and consider a polynomial $f(X) = a_n X^n + \dots + a_1 X + a_0 \in \mathbb{F}_{q^d}[X]$. Let β be a primitive element of the extension $\mathbb{F}_{q^d}/\mathbb{F}_q$, i.e., $\mathbb{F}_q(\beta) = \mathbb{F}_{q^d}$. For $i = 0, \dots, d-1$, define the following polynomials over \mathbb{F}_{q^d} :*

$$g_i := \sum_{j=0}^{d-1} \pi^j(\beta^i f).$$

Then $g_i(X) \in \mathbb{F}_q[X]$, and $\gcd(g_1, \dots, g_d)$ divides f . In particular, if $\gcd(g_1, \dots, g_d)$ is of degree 1, then f has a root in \mathbb{F}_q , and if $\gcd(g_1, \dots, g_d) = 1$, then $f(X)$ does not have any roots in \mathbb{F}_q .

Proof. Using the notation in Theorem 1, we have

$$\begin{aligned} g_i(X) &= [(\beta^i a_n + \pi(\beta^i a_n) + \dots + \pi^{d-1}(\beta^i a_n))X^n + \dots + (\beta^i a_0 + \dots + \pi^{d-1}(\beta^i a_0))] \\ &= \sum_{m=0}^n L_{\beta^i}(a_m) X^m. \end{aligned}$$

By Theorem 1, for all $i = 0, \dots, d-1$ we have $L_{\beta^i}(a_i) \in \mathbb{F}_q$, implying that $g_i(X) \in \mathbb{F}_q[X]$. Setting $A \in \text{GL}_d(\mathbb{F}_{q^d})$ to be

$$A = \begin{bmatrix} 1 & 1 & \dots & 1 \\ \beta & \pi(\beta) & \dots & \pi^{d-1}(\beta) \\ \vdots & \vdots & \ddots & \vdots \\ \beta^{d-1} & \pi(\beta^{d-1}) & \dots & \pi^{d-1}(\beta^{d-1}) \end{bmatrix} = \begin{bmatrix} 1 & 1 & \dots & 1 \\ \beta & \beta^q & \dots & \beta^{q^{d-1}} \\ \vdots & \vdots & \ddots & \vdots \\ \beta^{d-1} & (\beta^{d-1})^q & \dots & (\beta^{d-1})^{q^{d-1}} \end{bmatrix},$$

we have $(g_1, \dots, g_d) := A \cdot (f, \pi(f), \dots, \pi^{d-1}(f))$. As for Vandermonde matrices [14, §6.2], we find $\det(A) = \prod_{0 \leq i < j \leq d-1} (\beta^{q^j} - \beta^{q^i})$, which is non-zero for β a primitive element of the extension $\mathbb{F}_{q^d}/\mathbb{F}_q$. By Lemma 1, we have

$$\gcd(f, \pi(f), \dots, \pi^{d-1}(f)) = \gcd(g_1, \dots, g_d),$$

which gives that $\gcd(g_1, \dots, g_d) \mid f$. \square

Applying Proposition 1 to detect subfield nodes. Proposition 1 tells us that $\gcd(g_1, \dots, g_d)$ is precisely the largest divisor of $f \in \mathbb{F}_{q^d}[X]$ that is defined over $\mathbb{F}_q[X]$. In our target application of searching for subfield nodes in large supersingular isogeny graphs, i.e., when $d = 2$ and $q = p$, we will most commonly encounter $\gcd(g_1, g_2) = 1$, which immediately rules out subfield neighbours in the ℓ -isogeny graph. Non-trivial GCD's will, with overwhelmingly high probability, be of degree 1 and reveal a single subfield node; this is why our implementation of Algorithm 1 below terminates and returns `true` when the degree of the GCD is 1.

For large supersingular isogeny graphs, the only way for the degree of $\gcd(g_1, g_2)$ to be larger than 1 is when a given j -invariant is ℓ -isogenous to multiple subfield nodes, or when a given j -invariant is ℓ -isogenous to conjugate j -invariants in \mathbb{F}_{p^2} .⁷

In our scenario where $d = 2$, we see that $\pi(\beta) + \beta = 0$, meaning that $\pi^k(\beta) = (-1)^k \beta$. As a result, to detect a subfield root, we compute $\gcd(g_1, \beta g_2)$ where $g_1 = f + \pi(f)$ and $g_2 = f - \pi(f)$. In this case we do not need to calculate any more powers of β and we only need to do one GCD computation.

⁷A real-world attack should check any non-trivial GCD, since either of these scenarios are a win for the cryptanalyst; the latter case reveals information about the secret endomorphism ring of the target isomorphism class (see [16, §5.3]), and the former case gives multiple solutions to the subfield search problem.

Inversion-free polynomial GCD. To complete the detection of roots in a subfield, we must compute the GCD of polynomials in $K[X]$. In Algorithm 1, we modify Euclid’s polynomial-adapted algorithm [22, §17.3] to compute the GCD of two polynomials $g, h \in K[X]$ while avoiding inversions in K . We use $\text{LC}(f)$ to denote the leading coefficient of the polynomial f . Note that, for the purposes of incorporating it into our target application of subfield searching in the next section, the algorithm outputs the boolean `true` when the GCD has degree 1 in $K[X]$.

Algorithm 1 `InvFreeGCD()`: Inversion-free GCD

Input: Polynomials $g, h \in K[X]$, such that $\deg g \geq \deg h$

```

1: Initialise  $r, s \leftarrow \text{LC}(h) \cdot g, \text{LC}(g) \cdot h$ 
2: while  $\deg r \geq 1$  and  $r \neq s$  do
3:    $r \leftarrow r - X^{\deg r - \deg s} \cdot s$ 
4:    $r, s \leftarrow \text{LC}(s) \cdot r, \text{LC}(r) \cdot s$ 
5:   if  $\deg r < \deg s$  then
6:      $r, s \leftarrow s, r$ 
7:   end if
8: end while
9: return  $\neg(\deg r = 1 \text{ and } r \neq s)$ 

```

Proposition 2. *Given input $g, h \in K[X]$ such that $\deg g \geq \deg h$, Algorithm 1 terminates using at most*

$$\frac{1}{2}(\deg g + \deg h + 2)(\deg g + \deg h + 3) - 6$$

multiplications in K .

Proof. Line 1 incurs at most $\deg g + \deg h + 2$ multiplications in K . Setting $r_0 := r, s_0 := s$, we define this to be loop 0. For $i \geq 1$, we denote by r_i, s_i (where $\deg s_i \geq \deg r_i$) the polynomials in loop i of Lines 2-8. Using this notation, we move to Line 9 when $\deg r_i \leq 1$ or $r_i = s_i$. Now, in loop $i \geq 1$ we replace r_i by $r_i - X^{\deg r_i - \deg s_i} s_i$, meaning $\deg r_{i-1} - \deg r_i \geq 1$, and compute $r_i \cdot \text{LC}(s_i)$ and $s_i \cdot \text{LC}(r_i)$. This requires $\deg r_i + \deg s_i + 2$ multiplications in K . In the worst case, we have $\deg r_{i-1} - \deg r_i = 1$ for $i \geq 1$, where the number of multiplications will decrease by exactly 1 after each loop. In the final loop we have $\deg r_i, \deg s_i = 1$, so we compute 4 multiplications in K . In summary, in the worst case we begin with $\deg g + \deg h + 2$ multiplications, decreasing by 1 until we get to 4. Therefore, the total number of multiplications is at most $\sum_{n=4}^{\deg g + \deg h + 2} n$, which is the bound above. \square

In summary, Proposition 1 shows that detecting subfield roots of $f \in \mathbb{F}_{q^d}[X]$ amounts to computing the GCD of d related polynomials in $\mathbb{F}_q[X]$. We showed that computing this GCD is simpler when $d = 2$. Proposition 2 gives an upper bound on the number of \mathbb{F}_q multiplications required to compute such a GCD in $\mathbb{F}_q[X]$. In the next section we use these tools to build a faster algorithm for finding subfield nodes in supersingular isogeny graphs.

5 SuperSolver: optimised subfield searching with fast subfield root detection in $\mathcal{X}(\overline{\mathbb{F}}_p, \ell)$

SuperSolver is an algorithm which, given two j -invariants in S_{p^2} corresponding to two supersingular curves E_1/\mathbb{F}_{p^2} and E_2/\mathbb{F}_{p^2} , will, on average, solve the supersingular isogeny problem with lower concrete complexity than the traditional Delfs–Galbraith Solver algorithm described in Section 3. As in the Delfs–Galbraith algorithm, SuperSolver takes self-avoiding walks in $\mathcal{X}(\overline{\mathbb{F}}_p, 2)$ until they hit a j -invariant in \mathbb{F}_p . However, at each step of the random walk, SuperSolver also inspects

$\mathcal{X}(\overline{\mathbb{F}}_p, \ell)$, for carefully chosen $\ell > 2$, to efficiently detect whether j has any ℓ -isogenous neighbours in \mathbb{F}_p . Traditionally, inspecting $\mathcal{X}(\overline{\mathbb{F}}_p, \ell)$ for a subfield neighbour requires fully factoring a degree- N_ℓ polynomial and determining whether any of the roots lie in \mathbb{F}_p . Performing this for each ℓ would require $O(\ell^3 + 2\ell^2 \log p)$ operations in \mathbb{F}_{p^2} using the modified Cantor-Zassenhaus algorithm (see Section 2), which is prohibitively costly. Following the results from Section 4, however, **SuperSolver** conducts the inspection of $\mathcal{X}(\overline{\mathbb{F}}_p, \ell)$ with $O(\ell^2)$ multiplications in \mathbb{F}_p . We make this count precise later in this section. Crucially, the number of \mathbb{F}_p operations is no longer dependent on the size of p , and this means that as p grows large, the set of ℓ 's that are optimal to use also grows, and the more profitable (relatively speaking) **SuperSolver** becomes. We reiterate that, although both **Solver** and **SuperSolver** return the full isogeny between E_1/\mathbb{F}_{p^2} and E_2/\mathbb{F}_{p^2} , our discussion focusses on the bottleneck problem of finding an isogeny from E_1/\mathbb{F}_{p^2} (resp. E_2/\mathbb{F}_{p^2}) to E'_1/\mathbb{F}_p (resp. E_2/\mathbb{F}_p). If, at some node j , we detect an ℓ -isogenous neighbour in \mathbb{F}_p , **SuperSolver** will then factorise the degree- ℓ polynomial $\Phi_{\ell,p}(X, j)$ to determine the subfield j -invariant. We view this as a post-computation step, since we are only interested in the concrete complexity of the average step taken in the walk (which we assume does not find a subfield node). Note that the paths between E_1/\mathbb{F}_{p^2} and E_2/\mathbb{F}_{p^2} returned by both **Solver** and **SuperSolver** both look the same: in general, both start and finish with a chain of 2-isogenies that is connected in the middle by a chain of different prime-degree isogenies. The main difference, as the results in Section 7 illustrate, is that 2-isogeny chains at each end are *much* shorter. Recall that in the original Delfs–Galbraith algorithm, each step consists of finding the roots of a quadratic equation in $\mathbb{F}_{p^2}[X]$, which reveals two neighbouring nodes in $\mathcal{X}(\overline{\mathbb{F}}_p, 2)$. In **SuperSolver**, after forming a list of carefully chosen $\ell > 2$, each step will also include the rapid inspection of $\mathcal{X}(\overline{\mathbb{F}}_p, \ell)$ for every ℓ in this list. Though the inspection of the neighbours in $\mathcal{X}(\overline{\mathbb{F}}_p, \ell)$ increases the total number of \mathbb{F}_p multiplications at each step, more nodes are checked. We first describe the process of taking a step in **SuperSolver**, and then move to describing how to choose the list of $\ell > 2$ in order to minimise the number of \mathbb{F}_p multiplications per node inspected.

Remark 2 (Odd ℓ only). With the exception of the leaf nodes in the last level of the binary tree, it is redundant to perform rapid node inspections in $\mathcal{X}(\overline{\mathbb{F}}_p, 2\ell)$ if rapid inspections in $\mathcal{X}(\overline{\mathbb{F}}_p, \ell)$ are also part of the routine, since the latter inspections will detect (or exclude) subfield nodes at the next level of the walk down the tree. We therefore find it optimal to only include odd ℓ_i in the lists constructed at the end of this section. Note that there is no redundancy in including odd composite ℓ_i 's in our lists, even if they have proper divisors that are also in the list.

Rapid inspection of the ℓ -isogenous neighbours. Here we describe Algorithm 2: **Neighbour-InFp**. On input of $\ell, j \in \mathbb{F}_{p^2}$ and p , it outputs **true** if j is ℓ -isogenous to a $j' \in \mathbb{F}_p$, and **false** otherwise. Recall from Equation (1) that the degree of $\Phi_{\ell,p}$ in X and Y is N_ℓ . The first subroutine of **NeighbourInFp** is **EvalModPolyj**(ℓ, j, p): it evaluates $\Phi_{\ell,p}(X, Y)$ at $Y = j$ by computing j^2, \dots, j^{N_ℓ} , and then multiplying these by the corresponding coefficients of $\Phi_{\ell,p}$, returning the coefficients a_{N_ℓ}, \dots, a_0 of X in $\Phi_{\ell,p}(X, j)$. Note that, since we typically have a list of multiple ℓ , i.e., $\ell_1 < \dots < \ell_t$, the powers of j (up to N_{ℓ_t}) are computed once-and-for-all at every j , and recycled among the $\ell_i < \ell_t$. We follow Section 4 to detect whether $\Phi_{\ell,p}(X, j) \in \mathbb{F}_{p^2}[X]$ has a root in \mathbb{F}_p . Letting $\alpha \in \mathbb{F}_{p^2}$ be such that $\mathbb{F}_{p^2} = \mathbb{F}_p(\alpha)$, we first compute the related polynomials

$$\begin{aligned} g &:= (1/2) \cdot [\Phi_{\ell,p}(X, j) + \pi(\Phi_{\ell,p}(X, j))] && \text{and} \\ h &:= (-\alpha/2) \cdot [\Phi_{\ell,p}(X, j) - \pi(\Phi_{\ell,p}(X, j))], \end{aligned}$$

where $\pi \in \text{Gal}(\mathbb{F}_{p^2}/\mathbb{F}_p)$ is the Frobenius endomorphism. By Proposition 1, we have $g, h \in \mathbb{F}_p[X]$ and

$$\deg(\gcd(g, h)) = 1 \implies \Phi_{\ell,p}(X, j) \text{ has a root in } \mathbb{F}_p.$$

We then complete the inspection of $\mathcal{X}(\overline{\mathbb{F}}_p, \ell)$ by using Algorithm 1 to calculate $\gcd(g, h)$. If $\gcd(g, h) \neq 1$, then (for large enough p) it is overwhelmingly likely that $\deg(\gcd(g, h)) = 1$, which is why our implementation uses the degree of the GCD as the criterion for terminating the

subfield search. Another possibility is to terminate whenever $\gcd(g, h)$ is non-constant, and then to inspect the higher degree GCD according to the two possible scenarios discussed in Section 4.

Note that if we have a polynomial $f(X) = a_n X^n + a_{n-1} X^{n-1} + \dots + a_1 X + a_0 \in \mathbb{F}_{p^2}[X]$ then

$$\begin{aligned} \frac{1}{2}[f + \pi(f)] &= \operatorname{Re}(a_n)X^n + \operatorname{Re}(a_{n-1})X^{n-1} + \dots + \operatorname{Re}(a_1)X + \operatorname{Re}(a_0) \in \mathbb{F}_p[X], \\ \frac{-\alpha}{2}[f - \pi(f)] &= \operatorname{Im}(a_n)X^n + \operatorname{Im}(a_{n-1})X^{n-1} + \dots + \operatorname{Im}(a_1)X + \operatorname{Im}(a_0) \in \mathbb{F}_p[X], \end{aligned}$$

where, for $a + b\alpha \in \mathbb{F}_{p^2}$, $\operatorname{Re}(a + b\alpha) = a$ and $\operatorname{Im}(a + b\alpha) = b$, in analogy with the notation used for complex numbers. As a result, we can obtain g and h directly from f by computing

$$g = X^{N_\ell} + \dots + \operatorname{Re}(a_0), \quad \text{and} \quad h = \operatorname{Im}(a_{N_\ell-1})X^{N_\ell-1} + \dots + \operatorname{Im}(a_0).$$

This avoids having to compute any \mathbb{F}_{p^2} multiplications to calculate the related polynomials g, h .

Algorithm 2 `NeighbourInFp()`: Detect whether $j \in \mathbb{F}_{p^2}$ is ℓ -isogenous to a $j' \in \mathbb{F}_p$

Input: ℓ, j, p

- 1: $a_{\ell+1}, \dots, a_0 \leftarrow \operatorname{EvalModPolyj}(\ell, j, p)$
 - 2: $g \leftarrow X^{N_\ell} + \dots + \operatorname{Re}(a_0)$
 - 3: $h \leftarrow \operatorname{Im}(a_{N_\ell-1})X^{N_\ell-1} + \dots + \operatorname{Im}(a_0)$
 - 4: **return** `InvFreeGCD(g, h)`
-

Cost of Inspecting the ℓ -isogeny Graph. Evaluating $\Phi_{\ell,p}(X, Y)$ at $Y = j$ with `EvalModPolyj` requires at most $9N_\ell(N_\ell - 1)$ multiplications in \mathbb{F}_p , noting that one \mathbb{F}_{p^2} multiplication is equivalent to 3 \mathbb{F}_p multiplications. By Proposition 2, we compute `InvFreeGCD(g, h)` with at most $(2N_\ell + 1)(N_\ell + 1) - 6$ \mathbb{F}_p multiplications. Therefore, for a fixed ℓ , the cost of inspecting $\mathcal{X}(\mathbb{F}_p, \ell)$ is

$$\begin{aligned} \operatorname{cost}_\ell &= \frac{1}{N_\ell} [\#\mathbb{F}_p \text{ multiplications needed to inspect } \ell\text{-isogenous neighbours}] \\ &\leq \frac{1}{N_\ell} [11N_\ell^2 - 6N_\ell - 5], \end{aligned}$$

which depends only on ℓ . This means that, for each ℓ , cost_ℓ can be computed once for all primes. In Table 3 we present the ℓ with the lowest cost, ordering them by increasing cost_ℓ from left to right.

ℓ	3	5	7	11	13	9	17	19	23	29
N_ℓ	4	6	8	12	14	12	18	21	24	30
\mathbb{F}_p muls per node	16.3	24.5	32.6	48.8	56.8	58.5	72.8	80.9	96.9	120.9
ℓ	31	25	15	37	41	43	27	21	47	53
N_ℓ	32	30	24	38	42	44	36	32	48	54
\mathbb{F}_p muls per node	128.9	139.5	145.3	152.9	168.9	176.9	186.3	187.5	192.4	216.9

Table 3. The cost of inspecting ℓ -isogenous neighbours, cost_ℓ , for ℓ ordered by increasing cost from left to right.

The important takeaway from Table 3 is that the number of \mathbb{F}_p multiplications incurred by our algorithm does not grow with p . This count is fixed and depends only on ℓ . Looking back at the root solving algorithms in Section 2, we see a stark difference in expected performance. Those

algorithms have many constants hidden by the big- O , have a leading ℓ^3 term (compared to our ℓ^2 term), and, importantly, the number of field operations they incur grows as the field grows due to their implicit dependency on $\log p$. Moreover, as mentioned in Section 2, the complexities cited are for *probabilistic* root finding algorithms. Their deterministic variants have even worse complexities [22, §20.6].

Choosing the ℓ_i to minimise the cost of a step. We consider the cost of each step in SuperSolver, which we denote by the ratio

$$\text{cost} = \frac{\text{total \# of } \mathbb{F}_p \text{ multiplications}}{\text{total \# of nodes revealed}}. \quad (3)$$

The aim of this section is to describe how to choose to construct a list of ℓ_i that minimises the cost. Recall from in Table 3 that the ℓ 's that give the cheapest cost per node inspected are (from left to right)

$$[3, 5, 7, 11, 13, 9, 17, 19 \dots]. \quad (4)$$

We will use L_b to denote each list of ℓ_i and cost_{L_b} to denote the corresponding cost, where the bit representation of b specifies the set of ℓ 's from Equation (4); the least significant bit of b determines if 3 is included, the second least significant bit of b determines if 5 is included, and so on. For example, $L_0 = \{\}$, $L_2 = \{5\}$, and $L_{11} = \{3, 5, 7\}$. As each step will always include revealing 2 neighbours in $\mathcal{X}(\mathbb{F}_p, 2)$. For a node j we have

$$\begin{aligned} \text{total \# of } \mathbb{F}_p \text{ muls.} &\geq \# \mathbb{F}_p \text{ muls. needed to find roots of } \Phi_{2,p}(X, j); \\ \text{total \# of nodes revealed} &\geq 2. \end{aligned}$$

Here, equality holds only when we take the list to be L_0 , which corresponds to the original Delfs–Galbraith algorithm. Minimising the cost in Equation (3) is a non-trivial task. We first restrict the L_b to only contain ℓ such that $\text{cost}_\ell < \text{cost}_{L_0}$, otherwise it would be more advantageous to take another step by moving to a neighbouring node in $\mathcal{X}(\mathbb{F}_p, 2)$. We emphasise that cost_{L_0} grows with p , whereas cost_ℓ stays fixed. This signifies that the condition on ℓ becomes less restrictive as p increases. Suppose that, imposing this condition we get $L_b \subseteq [\ell_1, \dots, \ell_n]$. We then exhaust all $b < 2^n$, corresponding to subsets of $[\ell_1, \dots, \ell_n]$, to determine the L_b that minimise Equation (3). It is important to note that, as this optimisation depends only on the prime p , L_b can be determined in the precomputation.

6 A worked example

We now use a worked example to illustrate how the Solver and SuperSolver programs solve the supersingular isogeny problem, and to highlight the differences between them. Our SuperSolver suite is written in Sage/Python and a boolean variable `supersolver` specifies whether Solver or SuperSolver is used. For a prime p , and two supersingular j -invariants j_1 and j_2 defined over $\mathbb{F}_{p^2} = \mathbb{F}_p(\alpha)$, Solver is run by entering

```
Solver(p, j10, j11, j20, j21, false)
```

and SuperSolver is run by calling

```
Solver(p, j10, j11, j20, j21, true),
```

where `j10 = Re(j_1)`, `j11 = Im(j_1)` and similiary for `j20, j21`.

We picked

$$p = 2^{20} - 3,$$

the smallest of the primes from Table 4 (of Section 7), and generated two pseudo-random⁸ j -invariants in $S_{p^2} \setminus S_p$:

$$j_1 = 129007\alpha + 818380 \quad \text{and} \quad j_2 = 97589\alpha + 660383.$$

⁸We do this by taking long walks in $\mathcal{X}(\mathbb{F}_p, 3)$ away from a known subfield curve.

Preprocessing. The preprocessing phase of both programs starts by constructing the extension field $\mathbb{F}_{p^2} = \mathbb{F}_p(\alpha)$, where α^2 is the first non-square in the sequence $-1, -2, 2, -3, 3, \dots$. It then computes a list of constants for the Tonelli-Shanks subroutine, most notably the exponent $(p - 2^e - 1)/2^{e+1}$, where e is the maximum integer such that $2^e \mid (p - 1)$. This exponent is Scott’s ‘progenitor’ [21, p. 3], which essentially determines the complexity of \mathbb{F}_p square roots, and therefore of \mathbb{F}_{p^2} square roots. As a result, it determines the cost of taking a step in $\mathcal{X}(\overline{\mathbb{F}}_p, 2)$ – see Section 3. The preprocessing phase then computes a set of integers $\ell \geq 3$ (according to the optimisations in Section 5 and the relevant heuristics in [9]), fetches the associated files (originally from Sutherland’s database [24]) containing $\Phi_\ell(X, Y) \in \mathbb{Z}[X, Y]$ and reduces all of the coefficients to store a set of new, more compact files containing elements of \mathbb{F}_p that define each of the $\Phi_{\ell,p}(X, Y) \in \mathbb{F}_p[X, Y]$. Note that this is done for both *Solver* and *SuperSolver*, since both of these programs use the original Delfs–Galbraith subfield path algorithm [9, Algorithm 1] after the searches for subfield nodes is complete. It is important to note, especially in the cryptanalytic context, that all of these preprocessing steps only depend on p and can therefore be done without knowledge of j_1 and j_2 .

Solver. The optimised walk in $\mathcal{X}(\overline{\mathbb{F}}_p, 2)$ proceeds exactly as described in Section 3, i.e., using the depth first search through the binary trees rooted at j_1 and j_2 , until both searches find the subfield nodes $j'_1 \in \mathbb{F}_p$ and $j'_2 \in \mathbb{F}_p$. In the case of our example, paths were found to $j'_1 = 760776$ and $j'_2 = 946405$, depicted in Figure 2 and Figure 3. They correspond to $\phi_1: E_1 \rightarrow E'_1$ and $\phi_2: E_2 \rightarrow E'_2$, where $j(E_1) = j_1$, $j(E'_1) = j'_1$, $j(E_2) = j_2$, and $j(E'_2) = j'_2$.

$$\begin{array}{ccccccc}
\phi_1 : j_1 & \xrightarrow{2} & 219247\alpha + 863507 & \xrightarrow{2} & 489342\alpha + 132142 & & \\
& & & & \downarrow 2 & & \\
174188\alpha + 794346 & \xleftarrow{2} & 291380\alpha + 146098 & \xleftarrow{2} & 148602\alpha + 24450 & & \\
\downarrow 2 & & & & & & \\
263095\alpha + 184707 & \xrightarrow{2} & 37438\alpha + 90559 & \xrightarrow{2} & 1027930\alpha + 498080 & & \\
& & & & \downarrow 2 & & \\
612554\alpha + 208821 & \xleftarrow{2} & 994015\alpha + 681197 & \xleftarrow{2} & 206051\alpha + 982009 & & \\
\downarrow 2 & & & & & & \\
649416\alpha + 751358 & \xrightarrow{2} & 203489\alpha + 43055 & \xrightarrow{2} & 393773\alpha + 1028490 & & \\
& & & & \downarrow 2 & & \\
318158\alpha + 140927 & \xleftarrow{2} & 175225\alpha + 937858 & \xleftarrow{2} & 971263\alpha + 725197 & & \\
\downarrow 2 & & & & & & \\
348684\alpha + 935077 & \xrightarrow{2} & 341898\alpha + 405481 & \xrightarrow{2} & 274229\alpha + 367729 & & \\
& & & & \downarrow 2 & & \\
& & & & & & j'_1 = 760776
\end{array}$$

Fig. 2. A walk through $\mathcal{X}(\overline{\mathbb{F}}_p, 2)$ for $p = 2^{20} - 3$ during *Solver*. The walk starts at $j_1 = 129007\alpha + 818380 \in S_{p^2}$ and finds the subfield node $j'_1 = 760776 \in S_p$ after 21 steps.

Solver then computes a connecting path between the subfield nodes following Delfs–Galbraith [9, Algorithm 1]. This is depicted in Figure 4. *Solver* simply reverses the steps in ϕ_2 to obtain its dual, $\hat{\phi}_2$, and outputs the full path as $\phi: E_1 \rightarrow E_2$ as $\phi = \hat{\phi}_2 \circ \phi' \circ \phi_1$.

SuperSolver. With $p = 2^{20} - 3$, the preprocessing phase determined that *SuperSolver* is optimal with $L_3 = \{3, 5\}$ (see also Table 4 in the next section). Before departing the starting node $j_1 = 129007\alpha + 818380$, *SuperSolver* performs the rapid inspection of its 3- and 5-isogenous neighbours

$$\begin{array}{ccccccc}
\phi_2 : j_2 & \xrightarrow{2} & 867493\alpha + 220256 & \xrightarrow{2} & 252807\alpha + 1011175 & & \\
& & & & \downarrow 2 & & \\
657423\alpha + 286117 & \xleftarrow{2} & 440840\alpha + 706619 & \xleftarrow{2} & 953362\alpha + 11601 & & \\
\downarrow 2 & & & & & & \\
734841\alpha + 660440 & \xrightarrow{2} & 919529\alpha + 442520 & \xrightarrow{2} & 219960\alpha + 646080 & & \\
& & & & \downarrow 2 & & \\
638727\alpha + 940073 & \xleftarrow{2} & 219719\alpha + 594710 & \xleftarrow{2} & 619876\alpha + 961666 & & \\
\downarrow 2 & & & & & & \\
407014\alpha + 868179 & \xrightarrow{2} & 535787\alpha + 1046047 & \xrightarrow{2} & 138865\alpha + 8726 & & \\
& & & & \downarrow 2 & & \\
1016378\alpha + 696447 & \xleftarrow{2} & 289439\alpha + 170877 & \xleftarrow{2} & 665078\alpha + 700037 & & \\
\downarrow 2 & & & & & & \\
895198\alpha + 793471 & \xrightarrow{2} & 562302\alpha + 547814 & \xrightarrow{2} & 68076\alpha + 946405 & & \\
& & & & \downarrow 2 & & \\
& & & & j'_2 = 35387 & &
\end{array}$$

Fig. 3. A walk through $\mathcal{X}(\overline{\mathbb{F}}_p, 2)$ for $p = 2^{20} - 3$ during Solver. The walk starts at $j_2 = 97589\alpha + 660383 \in S_{p^2}$ and finds the subfield node $j'_2 = 35387 \in S_p$ after 21 steps.

$$\begin{array}{ccccccc}
\phi' : j'_1 & \xrightarrow{31} & 815910 & \xrightarrow{17} & 848568 & \xrightarrow{31} & 157399 & \xrightarrow{29} & 451011 & \xrightarrow{31} & 820763 & & \\
& & & & & & & & & & & \downarrow 31 & & \\
& & & & & & & & & & & j'_2 & \xleftarrow{17} & 286978 & \xleftarrow{37} & 76159 & &
\end{array}$$

Fig. 4. A path connecting two subfield j -invariants by taking steps in $\mathcal{X}(\overline{\mathbb{F}}_p, \ell)$ with $\ell \in \{17, 29, 31, 37\}$. The walk starts at $j'_1 = 760776 \in S_p$ and connects to $j'_2 = 35387 \in S_p$ after 8 steps.

as described in Section 5. It then takes steps in $\mathcal{X}(\overline{\mathbb{F}}_p, 2)$ as in Section 3, but at each new node it performs the rapid inspection of the 3- and 5-isogenous neighbours. In our example, both walks found a subfield node after 2 steps in $\mathcal{X}(\overline{\mathbb{F}}_p, 2)$. The walk from j_1 found a 3-isogenous neighbour and the walk from j_2 found a 5-isogenous neighbour. The final step that finds ϕ' is implemented in **SuperSolver** exactly as it was for **Solver**. The three isogenies ϕ_1 , ϕ_2 , and ϕ' , comprising the full isogeny $\phi = \hat{\phi}_2 \circ \phi' \circ \phi_1$, are depicted in Figure 5.

$$\begin{array}{l}
\phi_1 : j_1 \xrightarrow{2} 219247\alpha + 863507 \xrightarrow{2} 489342\alpha + 132142 \xrightarrow{3} j'_1 = 35387 \\
\phi_2 : j_2 \xrightarrow{2} 867493\alpha + 220256 \xrightarrow{2} 252807\alpha + 1011175 \xrightarrow{5} j'_2 = 292917 \\
\phi' : j'_1 \xrightarrow{17} 658300 \xrightarrow{29} 343840 \xrightarrow{31} 560315 \\
 \phantom{\xrightarrow{17}} \phantom{\xrightarrow{29}} \phantom{\xrightarrow{31}} \phantom{\xrightarrow{17}} \phantom{\xrightarrow{37}} \\
 \phantom{\xrightarrow{17}} \phantom{\xrightarrow{29}} \phantom{\xrightarrow{31}} \phantom{\xrightarrow{17}} \phantom{\xrightarrow{37}} \downarrow 17 \\
 \phantom{\xrightarrow{17}} \phantom{\xrightarrow{29}} \phantom{\xrightarrow{31}} \phantom{\xrightarrow{17}} \phantom{\xrightarrow{37}} j'_2 \xleftarrow{37} 439276
\end{array}$$

Fig. 5. The three paths found comprising an isogeny from E_1 to E_2 as found by **SuperSolver**.

To illustrate the core idea in this paper, we focus on the isogeny ϕ_1 depicted at the top of Figure 5 and walk through the steps of the **NeighbourInFp** algorithm. Evaluating the third modular polynomial at the intermediate j -invariants (Step 1 of Algorithm 2) yields

$$\begin{aligned}
\Phi_{3,p}(X, 219247\alpha + 863507) &= X^4 + (212814\alpha + 479338)X^3 + (408250\alpha + 920025)X^2 \\
&\quad + (811739\alpha + 93038)X + 942336\alpha + 847782; \\
\Phi_{3,p}(X, 489342\alpha + 132142) &= X^4 + (872004\alpha + 13960)X^3 + (1031755\alpha + 822066)X^2 \\
&\quad + (969683\alpha + 747785)X + 813010\alpha + 255391.
\end{aligned}$$

Though the theory tells us that these two polynomials split over $\mathbb{F}_{p^2}[X]$, to the naked eye there is no way to distinguish which (if any) of these polynomials has a root in \mathbb{F}_p . In both cases, setting $g = 1/2 \cdot (\Phi_{3,p} + \pi(\Phi_{3,p}))$ (Step 2 of Algorithm 2) and $h = -\alpha/2 \cdot (\Phi_{3,p} - \pi(\Phi_{3,p}))$ (Step 3 of Algorithm 2) respectively yields

$$\begin{aligned}
g &= X^4 + 479338X^3 + 920025X^2 + 93038X + 847782; \\
h &= 425628X^3 + 816500X^2 + 574905X + 836099,
\end{aligned}$$

and

$$\begin{aligned}
g &= X^4 + 13960X^3 + 822066X^2 + 747785X + 255391; \\
h &= 695435X^3 + 1014937X^2 + 890793X + 577447.
\end{aligned}$$

In the first case, Step 4 of Algorithm 2 outputs $\gcd(g, h) = 1$, meaning that $\Phi_{3,p}(X, 219247\alpha + 863507)$ has no subfield roots. In the second case, we see $\gcd(g, h) = X + 1013186$, meaning that $-1013186 = 35387$ is a subfield root. In our example, we note that the total number of steps between j_1 and j_2 returned by **SuperSolver** is 10, which is much shorter than the 50 steps taken by **Solver**. Since the middle subfield path finding algorithm is the same in both routines, there is no guarantee that the total path will always be smaller for **SuperSolver**. It is worth pointing out, however, that the two *outer* paths from elements in $S_{p^2} \setminus S_p$ to S_p (i.e., ϕ_1 and ϕ_2) returned by **SuperSolver** will never be longer than those returned by **Solver**. Indeed, **Solver** can be viewed as a special case of **SuperSolver** where the list of ℓ 's is chosen to be L_0 . Finally, we note that both **Solver** and **SuperSolver** always conclude by checking the correctness of the full path from j_1 to j_2 .

7 Implementation results

In this section we present some experimental results highlighting the efficacy of **SuperSolver**. The experiments focus solely on the search for subfield nodes (i.e., the bottleneck step of Delfs–Galbraith) and come in two flavours: many j -invariants over small primes, and one j -invariant over a large, cryptographic prime.

Small primes and many walks. Table 4 and Table 5 report experiments that were run on the largest primes of the 30 bitlengths from 20 to 49. We started at 5000 pseudo-random⁹ supersingular j -invariants in $S_{p^2} \setminus S_p$ for the primes of bitlengths 20–24, at 1000 j 's for the primes of bitlengths 25–29, at 500 j 's for the primes of bitlengths 30–34, at 100 j 's for the primes of bitlengths 35–39, at 50 j 's for the primes of bitlengths 40–44, and at 10 j 's for the primes of bitlengths 45–49. For every j , we ran both **Solver** and **SuperSolver** (with the five sets of ℓ 's that were predicted to perform best during preprocessing) until all walks hit a subfield j -invariant. Throughout, we will denote these fast sets of ℓ 's by L_b , as in Section 5. In all cases we counted the exact number of \mathbb{F}_p multiplications, squarings and additions required to find the subfield node. Following our metric in Section 2, Table 5 reports the average number of \mathbb{F}_p multiplications by counting squarings as multiplications, and highlights in **red** which of the five predicted sets of ℓ 's performed best on average.

Table 4 reports the average number of nodes visited in each of the walks, along with $\lceil \#S_{p^2} / \#S_p \rceil$, the expected number of random elements in S_{p^2} that would need to be sampled to find a subfield element in S_p . Here, the primes are small enough that S_p can be computed precisely (see Section 2). For each prime, Table 4 highlights in **red** the column that matches up with the least multiplications reported in Table 5. Note that, for **SuperSolver**, the number of nodes visited is the number of nodes that are actually walked onto in $\mathcal{X}(\overline{\mathbb{F}}_p, 2)$, not the number of nodes inspected using our fast subfield detection algorithm. Thus, in general, the lowest average number of nodes visited does not correspond to the lowest average number of multiplications. Indeed, the walks with fewer ℓ 's spend less compute inspecting ℓ -isogenous neighbours and therefore move onto new nodes faster, but do not cover as much of the supersingular set during the fast inspection.

The key trend to highlight is that, relatively speaking, **SuperSolver** gains more advantage over **Solver** as the primes get larger. This is not as evident for the small primes in Tables 4 and 5 as it is for the larger primes below.

Remark 3 ($\mathcal{X}(\mathbb{F}_p, 2)$ clusters in $\mathcal{X}(\overline{\mathbb{F}}_p, 2)$). An interesting trend to highlight in Table 4 is that the average number of nodes visited in the optimised Delfs–Galbraith walk through $\mathcal{X}(\overline{\mathbb{F}}_p, 2)$ is significantly more than the expected number of elements one would need to select randomly from S_{p^2} in order to find an element of S_p . The reason for this is that components of $\mathcal{X}(\mathbb{F}_p, 2)$ cluster together in $\mathcal{X}(\overline{\mathbb{F}}_p, 2)$ (see [7, Figure 3] for more details and a depiction). Thus, with respect to finding subfield nodes, walks in $\mathcal{X}(\overline{\mathbb{F}}_p, 2)$ are significantly different from selecting nodes at random from S_{p^2} . In general, this clustering does not happen in $\mathcal{X}(\overline{\mathbb{F}}_p, \ell)$ for $\ell > 2$, which seems to suggest that it may be preferable to perform the Delfs–Galbraith walk in a graph other than $\mathcal{X}(\overline{\mathbb{F}}_p, 2)$. However, we do not deem the difference between the number of nodes visited in $\mathcal{X}(\overline{\mathbb{F}}_p, 2)$ in practice and the theoretical expectation of $\lceil \frac{\#S_{p^2}}{\#S_p} \rceil$ great enough to incur the significant overhead of computing ℓ -th roots for any $\ell > 2$. In any case, the method of fast subfield root detection proposed in this paper will work regardless of the ℓ -isogenies that are used to take steps in a given walk. In fact, if it turns out that there is a larger ℓ that makes the original Delfs–Galbraith walk in $\mathcal{X}(\overline{\mathbb{F}}_p, \ell)$ perform faster than that of $\mathcal{X}(\overline{\mathbb{F}}_p, 2)$, the greater cost of taking a step in $\mathcal{X}(\overline{\mathbb{F}}_p, \ell)$ will increase the relative efficacy of invoking subfield root detection, and therefore the size of the set of fast ℓ 's.

⁹Just as in Section 6, we used long walks in $\mathcal{X}(\overline{\mathbb{F}}_p, 3)$ away from a known starting curve to achieve uniformity in S_{p^2} .

prime p	$\left\lceil \frac{\#S_{p^2}}{\#S_p} \right\rceil$	muls per step	fastest L_j 's $[L_{(i)} \dots, L_{(v)}]$	Average number of nodes visited					
				Solver DG	SuperSolver				
				$L_{(i)}$	$L_{(ii)}$	$L_{(iii)}$	$L_{(iv)}$	$L_{(v)}$	
$2^{20} - 3$	530	54	$[L_3, L_7, L_{11}, L_1, L_{15}]$	812	127	257	76	107	193
$2^{21} - 9$	156	53	$[L_3, L_7, L_1, L_5, L_{11}]$	459	86	218	53	87	111
$2^{22} - 3$	584	60	$[L_3, L_7, L_{15}, L_{11}, L_5]$	885	170	108	288	146	145
$2^{23} - 15$	583	71	$[L_7, L_3, L_{15}, L_{11}, L_5]$	838	172	106	169	121	430
$2^{24} - 3$	1277	64	$[L_3, L_7, L_{15}, L_{11}, L_5]$	1897	318	209	311	618	273
$2^{25} - 39$	1231	71	$[L_7, L_3, L_{15}, L_{11}, L_5]$	1873	360	223	359	933	259
$2^{26} - 5$	732	62	$[L_3, L_7, L_{15}, L_{11}, L_5]$	1362	352	194	691	271	233
$2^{27} - 39$	2348	73	$[L_7, L_3, L_{15}, L_{11}, L_5]$	3455	917	438	579	497	1766
$2^{28} - 57$	2965	64	$[L_3, L_7, L_{15}, L_{11}, L_5]$	9748	1788	1022	3065	1314	1306
$2^{29} - 3$	2953	74	$[L_7, L_3, L_{15}, L_{11}, L_{13}]$	4384	1053	526	712	603	2161
$2^{30} - 35$	3965	75	$[L_7, L_3, L_{15}, L_{11}, L_{13}]$	5555	1443	749	961	849	2825
$2^{31} - 1$	9009	75	$[L_7, L_3, L_{15}, L_{11}, L_{13}]$	27103	4501	2602	3755	3136	8794
$2^{32} - 5$	5142	77	$[L_7, L_3, L_{15}, L_{11}, L_{13}]$	10149	2520	1445	2108	1702	5335
$2^{33} - 9$	6638	75	$[L_7, L_3, L_{15}, L_{11}, L_{13}]$	20387	3832	2342	3756	2676	10562
$2^{34} - 41$	10526	78	$[L_7, L_3, L_{15}, L_{11}, L_{13}]$	32640	6443	3790	6094	4531	16320
$2^{35} - 31$	117571	99	$[L_{15}, L_7, L_{11}, L_3, L_{13}]$	150101	14893	27873	23076	20921	9850
$2^{36} - 5$	29040	83	$[L_7, L_{15}, L_3, L_{11}, L_{13}]$	63384	15929	9127	11974	10807	5249
$2^{37} - 25$	70328	84	$[L_7, L_{15}, L_3, L_{11}, L_{13}]$	218775	26241	16098	29226	24153	10405
$2^{38} - 45$	100268	86	$[L_7, L_{15}, L_3, L_{11}, L_{13}]$	217145	43595	21343	27187	26982	14897
$2^{39} - 7$	174817	96	$[L_7, L_{15}, L_{11}, L_3, L_{13}]$	230235	28802	48488	36770	38318	19677
$2^{40} - 87$	266662	95	$[L_7, L_3, L_5, L_6, L_{23}]$	394908	49855	80764	66646	56901	28016
$2^{41} - 21$	205227	92	$[L_7, L_3, L_5, L_6, L_{23}]$	44888	52656	105639	69940	62212	27395
$2^{42} - 11$	557046	99	$[L_7, L_3, L_5, L_6, L_{23}]$	720206	93920	189498	147651	102116	64309
$2^{43} - 57$	198777	95	$[L_7, L_3, L_5, L_6, L_{23}]$	705224	69021	153095	95778	81922	44112
$2^{44} - 17$	307870	98	$[L_7, L_3, L_5, L_6, L_{23}]$	808057	131220	285136	145263	142750	72964
$2^{45} - 55$	3120225	108	$[L_7, L_3, L_5, L_6, L_{23}]$	2298828	301730	410169	579449	404520	226542
$2^{46} - 21$	2759728	102	$[L_7, L_3, L_5, L_6, L_{23}]$	9075335	516826	788898	957832	730020	382101
$2^{47} - 115$	4234340	108	$[L_7, L_3, L_5, L_6, L_{23}]$	5182631	650377	866413	650377	801837	781907
$2^{48} - 59$	2706129	111	$[L_7, L_3, L_5, L_6, L_{23}]$	6739857	546014	899553	756358	651990	491312
$2^{49} - 81$	1239417	107	$[L_7, L_3, L_5, L_6, L_{23}]$	3582205	288124	660449	326050	319641	252270

Table 4. The average number of nodes visited in the search for subfield j -invariants in Solver and SuperSolver. Further explanation in text.

Large primes and optimal node coverage. Table 6 illustrates the increased efficacy of SuperSolver over Solver as the supersingular isogeny graphs get larger. Recall that we reported some of the results from this table up front in Section 1, namely from the experiments using primes from the isogeny literature. We chose the largest prime below 2^k for $k \in \{50, 100, \dots, 800\}$, and started from a pseudorandom j -invariant in $S_{p^2} \setminus S_p$ as usual. Since these instances are too large to actually run the full subfield search until it terminates, in each case we ran both Solver and SuperSolver (for the three sets of ℓ 's that were predicted to perform best during preprocessing) until the number of \mathbb{F}_p multiplications used exceeded 10^8 , and then immediately stopped. The numbers reported in bold in Table 6 are the total number of nodes covered (i.e., both walked onto *and* inspected) during these walks. For the smallest prime $p = 2^{50} - 27$, SuperSolver covers between 3 and 4 times the number of nodes that Solver does; for the largest prime $p = 2^{800} - 105$, SuperSolver covers between 18 and 19 times the number of nodes. Though primes beyond this size are unlikely to be of cryptographic interest, it is worth pointing out that this trend continues: the larger p grows, the more profitable it becomes to keep adding ℓ 's in the fast subfield inspection algorithm.

Storing and accessing the reduced modular polynomials. The unreduced modular polynomials $\Phi_\ell(X, Y) \in \mathbb{Z}[X, Y]$ require a significant amount of storage, but recall that the preprocessing phase immediately reduces all of the coefficients into \mathbb{F}_p to produce $\Phi_{\ell,p}(X, Y) \in \mathbb{F}_p[X, Y]$. This can be done once-and-for-all for a specific prime, and this makes the storage and access of the $\Phi_{\ell,p}(X, Y)$ a non-issue. Storing $\Phi_{\ell,p}(X, Y)$ requires at most $(N_\ell^2/2) \cdot \log_2(p)$ bits. For example, the largest $\Phi_{\ell,p}(X, Y)$ for the 250-bit prime above is $\Phi_{13,p}(X, Y)$, which requires the storage of at most $N_{13}^2/2 = 14^2/2 = 98$ elements of \mathbb{F}_p , around 3KB. The largest $\Phi_{\ell,p}(X, Y)$ for the 800-bit

prime p	$\left\lceil \frac{\#S_{p^2}}{\#S_p} \right\rceil$	muls per step	fastest L_j 's $[L_{(i)} \dots, L_{(v)}]$	Average number of \mathbb{F}_p multiplications					
				Solver DG	SuperSolver				
				$L_{(i)}$	$L_{(ii)}$	$L_{(iii)}$	$L_{(iv)}$	$L_{(v)}$	
$2^{20} - 3$	530	54	$[L_3, L_7, L_{11}, L_1, L_{15}]$	44848	20601	22585	22235	23459	24951
$2^{21} - 9$	156	53	$[L_3, L_7, L_1, L_5, L_{11}]$	24187	13648	18578	15453	18770	14064
$2^{22} - 3$	584	60	$[L_3, L_7, L_{15}, L_{11}, L_5]$	52385	28062	31962	26410	32555	38348
$2^{23} - 15$	583	71	$[L_7, L_3, L_{15}, L_{11}, L_5]$	59691	30508	32883	39703	33370	44556
$2^{24} - 3$	1277	64	$[L_3, L_7, L_{15}, L_{11}, L_5]$	112878	53900	62725	70482	59206	73117
$2^{25} - 39$	1231	71	$[L_7, L_3, L_{15}, L_{11}, L_5]$	128703	63021	68210	83333	94434	70878
$2^{26} - 5$	732	62	$[L_3, L_7, L_{15}, L_{11}, L_5]$	85437	59484	58286	65813	61261	62216
$2^{27} - 39$	2348	73	$[L_7, L_3, L_{15}, L_{11}, L_5]$	251304	164036	135672	136633	137780	185819
$2^{28} - 57$	2965	64	$[L_3, L_7, L_{15}, L_{11}, L_5]$	631157	305345	308003	298049	299314	351102
$2^{29} - 3$	2953	74	$[L_7, L_3, L_{15}, L_{11}, L_{13}]$	326888	199985	171489	173335	177986	235902
$2^{30} - 35$	3965	75	$[L_7, L_3, L_{15}, L_{11}, L_{13}]$	412457	260188	232753	228089	236360	301541
$2^{31} - 1$	9009	75	$[L_7, L_3, L_{15}, L_{11}, L_{13}]$	1998840	809040	807306	889210	871068	934319
$2^{32} - 5$	5142	75	$[L_7, L_3, L_{15}, L_{11}, L_{13}]$	758637	455571	449889	501335	474549	572203
$2^{33} - 9$	6638	77	$[L_7, L_3, L_{15}, L_{11}, L_{13}]$	1564701	700390	733705	900515	751310	1153911
$2^{34} - 41$	10526	78	$[L_7, L_3, L_{15}, L_{11}, L_{13}]$	2537688	1184024	1191084	1467113	1276654	1799292
$2^{35} - 31$	117571	99	$[L_{15}, L_7, L_{11}, L_3, L_{13}]$	15272705	5037679	5790782	6109529	6396752	6213090
$2^{36} - 5$	29040	83	$[L_7, L_{15}, L_3, L_{11}, L_{13}]$	5244914	3006618	2913909	2942626	3099020	3211580
$2^{37} - 25$	70328	84	$[L_7, L_{15}, L_3, L_{11}, L_{13}]$	18322417	4979176	5155517	7211517	6950196	6375918
$2^{38} - 45$	100268	86	$[L_7, L_{15}, L_3, L_{11}, L_{13}]$	18402937	8315681	6856578	6735588	7791309	9143526
$2^{39} - 7$	174817	96	$[L_7, L_{15}, L_{11}, L_3, L_{13}]$	22505327	9627241	9879376	9587856	11562406	12332858
$2^{40} - 87$	266662	95	$[L_7, L_3, L_5, L_6, L_{23}]$	38602102	16664021	16455546	17377853	17169885	17559520
$2^{41} - 21$	205227	92	$[L_7, L_3, L_5, L_6, L_{23}]$	41185437	17284297	20890068	17817383	18399209	17006068
$2^{42} - 11$	557046	99	$[L_7, L_3, L_5, L_6, L_{23}]$	70760036	31439715	38704883	38573868	30864574	40337712
$2^{43} - 57$	198777	95	$[L_7, L_3, L_5, L_6, L_{23}]$	66820000	22863425	30733754	24686759	24474388	27514948
$2^{44} - 17$	307870	98	$[L_7, L_3, L_5, L_6, L_{23}]$	79795521	43991657	58381667	38022655	43217829	45803624
$2^{45} - 55$	3120225	108	$[L_7, L_3, L_5, L_6, L_{23}]$	247697962	103871110	87674099	156886333	126109617	144250917
$2^{46} - 21$	2759728	102	$[L_7, L_3, L_5, L_6, L_{23}]$	923415913	174816651	163893709	198006728	205399202	220786555
$2^{47} - 115$	4234340	108	$[L_7, L_3, L_5, L_6, L_{23}]$	550653552	222915969	183895536	175113230	248769348	272706341
$2^{48} - 59$	2706129	111	$[L_7, L_3, L_5, L_6, L_{23}]$	729589278	188237971	192728454	205161765	251091015	310387211
$2^{49} - 81$	1239417	107	$[L_7, L_3, L_5, L_6, L_{23}]$	385982057	99186957	141171527	88278361	99648273	160633132

Table 5. The average number of \mathbb{F}_p multiplications used to search for subfield j -invariants in Solver and SuperSolver. Further explanation in text.

prime above requires the storage of at most $N_{19}^2/2 = 20^2/2 = 200$ elements of \mathbb{F}_p , around 20KB. Any of these would comfortably fit into the L1 cache on a modern CPU.

Concrete security of the supersingular isogeny problem. Our SuperSolver suite makes it straightforward to obtain precise estimates on the concrete classical security offered by the general supersingular isogeny problem in S_{p^2} , for any prime p . Combining a small experiment (like those reported in Table 6) with the expected number of nodes one must cover before reaching a subfield node allows us to obtain accurate counts on the expected number of \mathbb{F}_p multiplications, squarings and additions that must be carried out during a full cryptanalytic attack. It is then a matter of costing these \mathbb{F}_p operations with respect to the appropriate metric, whether that be bit operations, cycle counts, gate counts, or circuit depth.

Acknowledgements. Thanks to Sam Frengley, Michael Naehrig, Krijn Reijnders, Benjamin Smith, and Greg Zaverucha for their valuable comments on an earlier version of this paper, and to Drew Sutherland for answering our questions about alternative modular functions.

References

1. G. Adj and F. Rodríguez-Henríquez. Square root computation over even extension fields. *IEEE Transactions on Computers*, 63(11):2829–2841, 2013.
2. E. R. Berlekamp. Factoring polynomials over large finite fields. *Mathematics of computation*, 24(111):713–735, 1970.

prime p	Solver	SuperSolver		
$2^{50} - 27$	882,999 (113)	$\{3,5,7\}$ 2,859,201 (35.0)	$\{3,5\}$ 2,736,613 (36.5)	$\{3,7\}$ 2,533,945 (39.4)
$2^{100} - 15$	443,951 (223)	$\{3,5,7\}$ 2,165,681 (46.0)	$\{3,5,7,11\}$ 2,121,313 (47.8)	$\{3,5,7,11,9\}$ 2,006,215 (49.7)
$2^{150} - 3$	317,209 (315)	$\{3,5,7,11\}$ 1,895,169 (52.8)	$\{3,5,7,11,13\}$ 1,852,237 (54.0)	$\{3,5,7,11,9\}$ 1,847,371 (54.1)
$2^{200} - 75$	241,989 (415)	$\{3,5,7,11,13\}$ 1,716,767 (58.3)	$\{3,5,7,11,13,9\}$ 1,715,449 (58.4)	$\{3,5,7,11,9\}$ 1,700,791 (58.9)
$2^{250} - 207$	191,115 (526)	$\{3,5,7,11,13,9\}$ 1,607,145 (62.3)	$\{3,5,7,11,13\}$ 1,586,495 (63.2)	$\{3,5,7,11,9\}$ 1,561,645 (64.2)
$2^{300} - 153$	164,275 (609)	$\{3,5,7,11,13,9\}$ 1,531,993 (65.3)	$\{3,5,7,11,13\}$ 1,498,175 (66.8)	$\{3,5,7,11,13,9,17\}$ 1,489,991 (67.1)
$2^{350} - 113$	141,097 (708)	$\{3,5,7,11,13,9\}$ 1,452,529 (68.8)	$\{3,5,7,11,13,9,17\}$ 1,432,345 (69.8)	$\{3,5,7,11,13\}$ 1,406,543 (71.1)
$2^{400} - 593$	123,649 (809)	$\{3,5,7,11,13,9\}$ 1,380,849 (72.4)	$\{3,5,7,11,13,9,17\}$ 1,378,991 (72.5)	$\{3,5,7,11,13,9,17,19\}$ 1,346,081 (74.3)
$2^{450} - 501$	110,407 (907)	$\{3,5,7,11,13,9,17\}$ 1,332,176 (75.2)	$\{3,5,7,11,13,9\}$ 1,321,701 (75.9)	$\{3,5,7,11,13,9,17,19\}$ 1,316,198 (76.4)
$2^{500} - 863$	97,510 (1032)	$\{3,5,7,11,13,9,17\}$ 1,280,243 (78.6)	$\{3,5,7,11,13,9,17,19\}$ 1,274,001 (79.0)	$\{3,5,7,11,13,9\}$ 1,251,602 (80.4)
$2^{550} - 5$	90,321 (1111)	$\{\{3,5,7,11,13,9,17\}\}$ 1,243,309 (80.6)	$\{\{3,5,7,11,13,9,17,19\}\}$ 1,240,916 (80.7)	$\{3,5,7,11,13,9,19\}$ 1,216,189 (82.6)
$2^{600} - 95$	81,544 (1232)	$\{3,5,7,11,13,9,17,19\}$ 1,203,358 (83.3)	$\{3,5,7,11,13,9,17\}$ 1,198,900 (84.0)	$\{3,5,7,11,13,9,19\}$ 1,170,561 (85.8)
$2^{650} - 611$	76,569 (1311)	$\{3,5,7,11,13,9,17,19\}$ 1,184,513 (85.0)	$\{3,5,7,11,13,9,17\}$ 1,161,998 (86.1)	$\{3,5,7,11,13,9,17,19,23\}$ 1,144,708 (87.4)
$2^{700} - 1113$	71,037 (1409)	$\{3,5,7,11,13,9,17,19\}$ 1,148,963 (82.5)	$\{3,5,7,11,13,9,17\}$ 1,127,317 (82.6)	$\{3,5,7,11,13,9,17,19,23\}$ 1,123,125 (82.9)
$2^{750} - 161$	66,239 (1510)	$\{3,5,4,7,11,13,9,8,17,19,6\}$ 1,121,045 (84.4)	$\{3,5,4,7,11,13,9,8,17,19\}$ 1,101,767 (84.4)	$\{3,5,4,7,11,13,9,8,17,6\}$ 1,093,351 (85.1)
$2^{800} - 105$	62,191 (1609)	$\{3,5,4,7,11,13,9,8,17,19,6\}$ 1,096,056 (86.1)	$\{3,5,4,7,11,13,9,8,17,19\}$ 1,082,072 (86.3)	$\{3,5,4,7,11,13,9,8,17,6\}$ 1,062,658 (87.2)

Table 6. The number of nodes inspected per 10^8 field multiplications for the largest primes of various bitlengths. The Solver column corresponds to optimised Delfs–Galbraith walks in $\mathcal{X}(\mathbb{F}_p, 2)$ – see Section 3. The SuperSolver columns correspond to enabling our fast subfield root detection algorithm with the three fastest sets of ℓ 's (left to right) – see Section 5. Numbers in round brackets are the approximate number of \mathbb{F}_p multiplications per node inspected, as computed during the precomputation phase that determines which sets of ℓ 's will perform fastest.

3. W. Beullens, T. Kleinjung, and F. Vercauteren. CSI-FiSh: Efficient isogeny based signatures through class group computations. In S. D. Galbraith and S. Moriai, editors, *ASIACRYPT 2019*, volume 11921 of *Lecture Notes in Computer Science*, pages 227–247. Springer, 2019.
4. J. H. Bruinier, K. Ono, and A. V. Sutherland. Class polynomials for nonholomorphic modular functions. *Journal of Number Theory*, 161:204–229, 2016.
5. D. G. Cantor and H. Zassenhaus. A new algorithm for factoring polynomials over finite fields. *Mathematics of Computation*, pages 587–592, 1981.
6. C. Costello. B-SIDH: supersingular isogeny Diffie-Hellman using twisted torsion. In *ASICRYPT*, pages 440–463. Springer, 2020.
7. C. Costello, P. Longa, M. Naehrig, J. Renes, and F. Virdia. Improved classical cryptanalysis of SIKE in practice. In A. Kiayias, M. Kohlweiss, P. Wallden, and V. Zikas, editors, *PKC 2020*, volume 12111 of *Lecture Notes in Computer Science*, pages 505–534. Springer, 2020.
8. C. Costello, M. Meyer, and M. Naehrig. Sieving for twin smooth integers with solutions to the Prouhet-Tarry-Escott problem. In *EUROCRYPT*, volume 12696, pages 272–301. Springer, 2021.
9. C. Delfs and S. D. Galbraith. Computing isogenies between supersingular elliptic curves over \mathbb{F}_p . *Designs, Codes and Cryptography*, 78(2):425–440, 2016.
10. L. De Feo, D. Jao, and J. Plût. Towards quantum-resistant cryptosystems from supersingular elliptic curve isogenies. *J. Math. Cryptol.*, 8(3):209–247, 2014.
11. L. De Feo, D. Kohel, A. Leroux, C. Petit, and B. Wesolowski. SQISign: compact post-quantum signatures from quaternions and isogenies. In *ASIACRYPT*, pages 64–93. Springer, 2020.
12. S. D. Galbraith, C. Petit, and J. Silva. Identification protocols and signature schemes based on supersingular isogeny problems. *J. Cryptol.*, 33(1):130–175, 2020.

13. M. Hamburg. Fast and compact elliptic-curve cryptography. Cryptology ePrint Archive, Report 2012/309, 2012. <https://ia.cr/2012/309>.
14. R. A. Horn and C. R. Johnson. *Topics in matrix analysis*. Cambridge university press, 1994.
15. D. Jao, R. Azarderakhsh, M. Campagna, C. Costello, L. De Feo, B. Hess, A. Jalali, B. Koziel, B. LaMacchia, P. Longa, M. Naehrig, J. Renes, V. Soukharev, and D. Urbanik. SIKE: Supersingular Isogeny Key Encapsulation. Manuscript available at sike.org/, 2017.
16. C. Leonardi. *Security Analysis of Isogeny-Based Cryptosystems*. PhD thesis, University of Waterloo, Ontario, Canada, 2020.
17. R. Lidl and H. Niederreiter. *Introduction to finite fields and their applications*. Cambridge University Press, 1994.
18. A. J. Menezes, P. C. Van Oorschot, and S. A. Vanstone. *Handbook of applied cryptography*. CRC press, 2018.
19. J-F. Mestre. La méthode des graphes. exemples et applications. In *Proceedings of the international conference on class numbers and fundamental units of algebraic number fields (Katata)*, pages 217–242. Citeseer, 1986.
20. A. K. Pizer. Ramanujan graphs and Hecke operators. *Bulletin of the American Mathematical Society*, 23(1):127–137, 1990.
21. M. Scott. A note on the calculation of some functions in finite fields: Tricks of the trade. *IACR Cryptol. ePrint Arch.*, page 1497, 2020.
22. V. Shoup. *A computational introduction to number theory and algebra*. Cambridge university press, 2009.
23. J. H. Silverman. *The arithmetic of elliptic curves*, volume 106. Springer, 2009.
24. A. V. Sutherland. Modular Polynomials. <https://math.mit.edu/~drew/ClassicalModPolys.html>. Online; accessed 30 September 2021.
25. A. V. Sutherland. On the evaluation of modular polynomials. *The Open Book Series*, 1(1):531–555, 2013.
26. The Sage Developers. *SageMath, the Sage Mathematics Software System (Version x.y.z)*, YYYY. <https://www.sagemath.org>.
27. J. Vélu. Isogénies entre courbes elliptiques. *CR Acad. Sci. Paris Sér. AB*, 273(A238-A241):5, 1971.